

Effect of magnetism and temperature on the stability of $(\text{Cr}_x, \text{V}_{1-x})_2\text{AlC}$ phasesJoás Grossi,^{1,2} Shafqat H. Shah,³ Emilio Artacho,^{2,4,5} and Paul D. Bristowe³¹Facultad de Ciencias Exactas y Naturales, Universidad Nacional de Cuyo, Mendoza, 5500 Argentina²Theory of Condensed Matter, Cavendish Laboratory, University of Cambridge, J. J. Thomson Ave, Cambridge CB3 0HE, United Kingdom³Department of Materials Science and Metallurgy, University of Cambridge, 27 Charles Babbage Rd, Cambridge CB3 0FS, United Kingdom⁴CIC Nanogune and DIPC, Tolosa Hiribidea 76, 20018 San Sebastián, Spain⁵Basque Foundation for Science Ikerbasque, 48013 Bilbao, Spain

(Received 16 July 2018; revised manuscript received 28 October 2018; published 26 December 2018)

The stability of $(\text{Cr}_x, \text{V}_{1-x})_2\text{AlC}$ MAX phases, materials of interest for a variety of magnetic as well as high-temperature applications, has been studied using density-functional-theory first-principles calculations. The enthalpy of mixing predicts these alloys to be unstable towards unmixing at 0 K. The calculations also predict, however, that these phases would be thermally stabilized by configurational entropy at temperatures well below the values used for synthesis. The temperature T_s below which they become unstable is found to be quite sensitive to the presence of magnetic moments on Cr ions, as well as to the material's magnetic order, in addition to chemical order and composition. Allowing for magnetism, the value of T_s for $(\text{Cr}_{0.5}, \text{V}_{0.5})_2\text{AlC}$ with chemically disordered Cr and V atoms is estimated to be between 516 and 645 K depending on the level of theory, while if constrained to spin paired, T_s drops to ~ 142 K. Antiferromagnetic spin arrangements are found to be favored. The combination of antiferromagnetic frustration and configurational disorder should give rise to interesting spin textures at low temperatures.

DOI: [10.1103/PhysRevMaterials.2.123603](https://doi.org/10.1103/PhysRevMaterials.2.123603)

I. INTRODUCTION

There has been increasing interest in a class of ternary layered carbides and nitrides called MAX phases [1,2]. Their general chemical formula is $M_{n+1}AX_n$ where $n = 1-3$, M is an early transition metal, A is an A-group element, and X is most often carbon but sometimes nitrogen. At least 80 examples are known [3,4], and the number is steadily growing in a context of very active research [5-9], which is expanding their chemical space (see, e.g. the remarkable recent MAX phases incorporating noble metals [9]). Structurally, they are hexagonal and can be described as an array of edge-sharing MX_6 octahedra separated by close-packed layers of A atoms. The spacing between the A layers and the size of the octahedral array is determined by n . Strong $M-X$ bonds are present and to a lesser extent $A-X$ bonds. The combined effects of crystallography and interatomic bonding result in a number of unique physical and chemical properties such as good machinability, corrosion resistance, high electrical conductivity, and tolerance to radiation damage that make MAX phases potential candidates for a wide range of applications [10-22].

One particular property that has received increasing attention is magnetism, mainly due to the possibility of incorporating magnetic elements into the M layers and the prospect of creating multilayer spintronic devices [23,24]. Many of the studies performed to date, either theoretical or experimental, have focused on the introduction of transition metal elements which exhibit strong $3d$ electron correlation effects, such as Fe, Mn, or Cr, in an attempt to create spin configurations that exhibit magnetic order [25-31]. From a theoretical point of view, it is worth noting that the appearance of magnetic moments greatly affects properties beyond magnetic, such as,

e.g., the elastic constants calculated from first principles for Cr_2AlC , which deviate from experimental values by more than 25% if spin polarization is not allowed [32-35], but become much more accurate when including it [36-38].

However, the properties and thermodynamic stability of MAX phases can be altered by incorporating further elements into their structure, and this is most often done by substitution on the M site. This may be beneficial from both the phase stability and magnetic points of view. To this end, and with magnetism in mind, a number of measurements and calculations have been made on $(\text{Cr}, \text{Mn})_2\text{XC}$ ($X = \text{Al}, \text{Ge},$ or Ga) quaternary carbide phases resulting in some cases in the prediction of weak ferromagnetism at low temperatures [39-46]. Another possible candidate is the $(\text{Cr}_x, \text{V}_{1-x})_2\text{AlC}$ ($0 \leq x \leq 1$) solid solution series which has been synthesized [47-50] but not completely characterized magnetically. While several studies have been made on the end members of this series including phase stability, magnetism, and point defect formation [26,51-55], no systematic investigation of magnetic order has been made over the entire composition range.

The end member that has received most attention is Cr_2AlC . Recent measurements of its magnetic order have interpreted the spin configuration as very weak ferromagnetic (FM) [56] or canted antiferromagnetic (AFM) [57]. This has not been experimentally resolved yet. However, from the theoretical point of view, several groups have searched for possible spin-polarized Cr atoms in Cr_2AlC using first-principles density-functional-theory (DFT) calculations in attempts to identify its ground state. Considering a small set of FM, AFM, and nonmagnetic (NM) configurations within a single unit cell, a NM solution has been predicted for this material [32,58]. However allowing for unit-cell doubling, AFM

configurations with antiparallel spins of Cr atoms within the basal plane, were found to be energetically favorable [37,38]. In addition, DFT+ U calculations, using the onsite Coulomb repulsion U for localized Cr $3d$ electrons [36–38,59], were able to stabilize the same magnetic ground states of the AFM configurations and also a FM ground state within a single unit cell. In fact, the AFM configurations were found to be the most stable phases with or without $+U$ corrections. The observed Curie temperature $T_C \sim 73$ K [56] for Cr_2AlC would seem to indicate that magnetic effects should not be relevant to the stability of the $(\text{Cr}_x\text{V}_{1-x})_2\text{AlC}$ system at temperatures of interest, mainly room or synthesis temperature. We will see below that this is not the case.

The other end member is V_2AlC for which a NM solution has been predicted [37,60] from first principles. This appears to be consistent with recent measurements which suggest that it is a Pauli paramagnet up to room temperature [61].

The present contribution deals with chemically ordered and disordered quaternary $(\text{Cr}_x\text{V}_{1-x})_2\text{AlC}$ phases for $x = 0; 0.25; 0.5; 0.75; 1.0$. These phases are normally synthesized at temperatures between 1673 and 1873 K [47] by reactive sintering or hot isostatic pressing. This work aims to provide a theoretical evaluation on the phase stability and magnetic properties of these alloys using first-principles calculations.

II. METHOD

Ab initio calculations based on density functional theory [62,63] were performed using the SIESTA program [64]. We adopted the generalized gradient approximation (GGA) as parametrized by Perdew-Burke-Ernzerhof (PBE) [65] for treating electron exchange and correlation effects. All structural relaxations were done using the conjugate gradient method [66], to within a force tolerance of 0.02 eV/Å and a stress tolerance of 0.01 GPa. Integrations in real space were performed using a real-space grid with a 300 Ry mesh cutoff. For the k -point sampling of the Brillouin zone, values between

20–25 Å were used for the k -grid cutoff length [67] depending on each alloy.

Core electrons were replaced by pseudopotentials [64]. Two different valence configurations were considered in order to generate Cr and V pseudopotentials: the first configuration (fs) taken as $\text{Cr}(3p^63d^54s^1)$, $\text{V}(3p^63d^34s^2)$ and the second configuration (ss) taken as $\text{Cr}(3s^23p^63d^5)$, $\text{V}(3s^23p^63d^3)$. For Al and C pseudopotential generation, valences were taken as $\text{Al}(3s^23p^{0.5}3d^{0.5})$, $\text{C}(2s^22p^2)$. In addition, Kohn-Sham eigenvectors were expanded in atomiclike orbitals and basis sets were chosen to be the solutions of the pseudoatomic problem. Three basis sets were defined for Cr and V according to the valence configurations given above and denoted DZP, DZP+P($3d$) and TZ2P+P($3d$). For Al and C, a DZP basis set was chosen for each. More detailed information on the basis sets and pseudopotentials can be found in Appendix A.

Figure 1 shows single unit cells of $(\text{Cr}_x\text{V}_{1-x})_2\text{AlC}$ ($x = 0; 0.25; 0.5; 0.75; 1.0$) for structures which are chemically ordered in layers along the c direction. Each unit cell contains eight atoms. To simulate the effects of M -site disorder, two further cells were considered focusing on the equiatomic composition CrVAIC ($x = 0.5$). One was modeled using the special quasirandom structure method [68] using a $4 \times 4 \times 1$ supercell containing 64 M sites and denoted SQSCrV. The other was modeled using a $2 \times 1 \times 1$ supercell with a total of eight M sites and denoted VVCrCr(CrV)(VCr). This structure is shown in Table IV of Appendix B.

Nonmagnetic (NM) calculations (following the nomenclature of previous papers on the topic) refer to spin-paired or non-spin-polarized DFT calculations. They should not be confused with paramagnetism, which allows for the presence of disordered magnetic moments. DFT calculations allowing for magnetic moments (spin polarized) are performed in this work for various spin arrangements, for $x = 0, 0.5$, and 1. The different arrangements found as most stable for the different mixing configurations explored in this work all give zero total magnetization, and will be generally referred to as AFM,

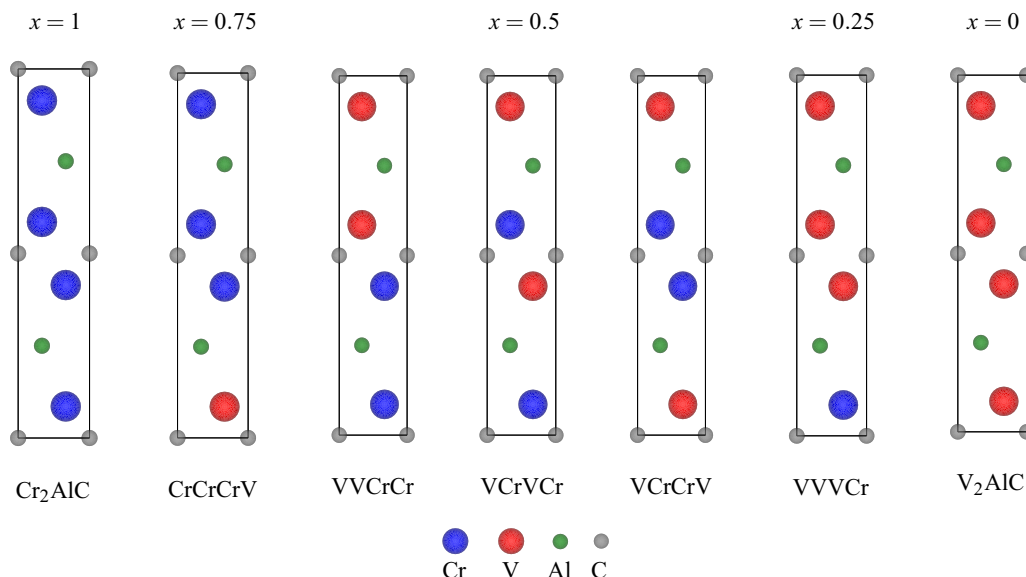


FIG. 1. Single $1 \times 1 \times 1$ unit cells of the ordered structures considered for $(\text{Cr}_x\text{V}_{1-x})_2\text{AlC}$. The vertical direction points along the c axis.

following the literature, although the structure defined by the Cr atoms is never bipartite and all configurations contain a certain degree of frustration. The particular arrangements obtained are not trivial, and are specified for $x = 0.5$ in Table IV of Appendix B. The most stable spin configuration for the Cr end member coincides with what found in previous works on that material [37,38], where it is called in-AFM1. Ferromagnetic (FM) configurations were also obtained but always found to be of significantly higher energy, and are therefore not reported in this work. Finally, the rotationally invariant approach to GGA+ U as proposed by Dudarev [69] was applied to describe the Cr 3d electrons (see Appendix B for the parameters used in the definition of the Hamiltonian).

The Gibbs free energy of mixing ΔG_{mix} for each alloy is expressed as

$$\Delta G_{\text{mix}} = \Delta H_{\text{mix}} - T \Delta S_{\text{mix}}, \quad (1)$$

where ΔH_{mix} is the enthalpy of mixing given by

$$\Delta H_{\text{mix}} = \Delta E_{\text{mix}} + p \Delta V_{\text{mix}} \quad (2)$$

for a given pressure p , and where ΔS_{mix} , ΔE_{mix} , and ΔV_{mix} are the mixing entropy, internal energy, and volume, respectively, each one of them defined as

$$\Delta \Omega_{\text{mix}} = \Omega_{\text{mixed}} - \Omega_{\text{pure1}} - \Omega_{\text{pure2}} \quad (3)$$

for $\Omega = S$, E , and V , respectively, all of them expressed per unit cell henceforth.

We expect the configurational entropy ΔS_c to be the main component of the total entropy of mixing since changes in vibrational entropy are expected to be small in comparison: the replacement of one M -site transition metal atom by another with very similar mass and chemistry should not change the phonon frequencies of the different phases enough so as to significantly affect the mixing entropy. In similar-mass situations, the vibrational contribution to the entropy of mixing in alloys is normally below $\sim 0.2 k_B/\text{atom}$ [70] (see, e.g., the case of FeCr alloys [71]). It is also quite systematically positive, in the direction of stabilizing the disordered alloys. In this sense, the stabilization temperatures discussed below can be taken as overestimations, the disordered alloys remaining stable to even lower temperatures than quoted. We also expect the configurational entropy to dominate over spin disorder entropy in ΔS_{mix} . The spin disorder contribution is zero in the limit of uncorrelated spins (there is an entropy of $k_B \ln 2$ per spin for both the alloy and the end-member phases, giving a net zero to the excess entropy of mixing). Spin-spin correlations can introduce a small correction, again in the direction of stabilizing the disordered phase (the spins of a Cr ion will correlate most with neighboring Cr spins, which means that the Cr end member will display larger correlations and therefore have a smaller spin entropy than the alloy).

The internal energy of mixing will be calculated at 0 K in this work since the variation with temperature is also expected to be sufficiently small to be negligible for present purposes. Finally, concerning the pV term, there are two synthesis processes for these materials [47]: one is at 0.1 MPa and the other one involves a pressure of 80 MPa which makes $p\Delta V$ less than 2 meV per unit cell for a $\Delta V < 3\%$ in all cases.

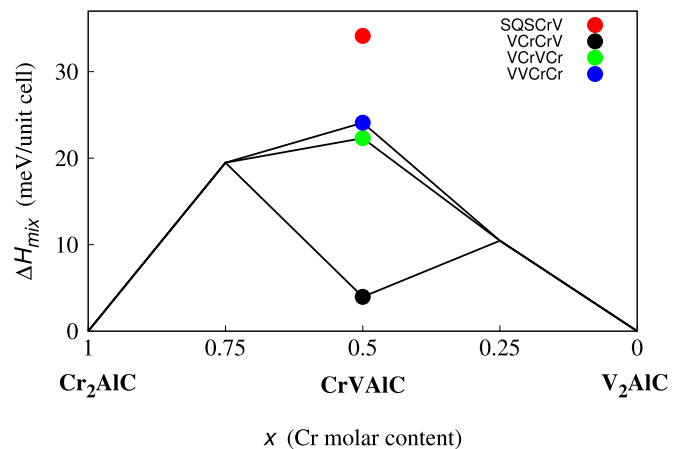


FIG. 2. Enthalpy of mixing ΔH_{mix} for the chemically ordered structures of $(\text{Cr}_x\text{V}_{1-x})_2\text{AlC}$ shown in Fig. 1 as a function of x . The enthalpy for the disordered structure SQSCrV at $x = 0.5$ is also shown. All configurations have been taken to be NM.

Thus, the resulting expression used to calculate the enthalpy of mixing for each alloy was

$$\Delta H_{\text{mix}} = E[(\text{Cr}_x\text{V}_{1-x})_2\text{AlC}] - x E(\text{Cr}_2\text{AlC}) - (1-x) E(\text{V}_2\text{AlC}), \quad (4)$$

where E is the internal energy of the corresponding phase.

The configurational entropy ΔS_c per unit cell of an ideal solid solution of V and Cr atoms on the M sites has the form

$$\Delta S_c = -y k_B [x \ln(x) + (1-x) \ln(1-x)], \quad (5)$$

where y is the number of M sites per unit cell, i.e., $y = 4$ and x is the Cr molar content. When $x = 0.5$, for example, $\Delta S_c = -23.89 \times 10^{-5} \text{ eV/K}$. Deviations from the ideal mixing behavior are not considered in this work.

The following section describes results obtained using the pseudopotentials associated to the fs valence configurations and DZP+P(3d) basis sets for Cr and V. Appendix A shows that using the ss valence configurations or the other basis sets has only a small effect on the enthalpy of mixing.

III. RESULTS

Figure 2 shows ΔH_{mix} as a function of composition for the chemically ordered structures with $x = 0; 0.25; 0.5; 0.75; 1.0$. Also plotted, for comparison, is ΔH_{mix} for the disordered SQSCrV structure at $x = 0.5$. First, all configurations have been taken to be nonmagnetic. It is seen that the enthalpies are all positive, resulting in a concave hull and therefore indicating that each configuration is unstable with respect to decomposition into the end members at 0 K. At $x = 0.5$, VCrCrV is the least unstable structure whereas SQSCrV is the most unstable structure.

To determine the effect of magnetism and magnetic order on ΔH_{mix} we have performed spin-polarized calculations focusing on the $x = 0.5$ equiatomic composition. In addition, DFT+ U has been employed to see whether the onsite Coulomb interactions of the localized 3d electrons of Cr influence the results. In previous studies [37,38] an antiferromagnetic state (in-AFM1) was found to be the ground state

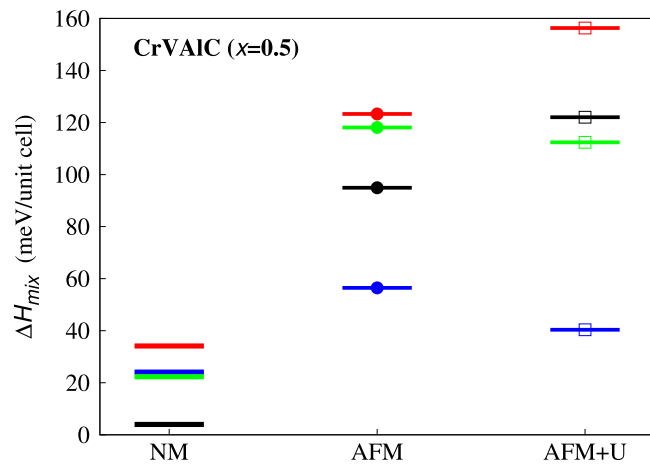


FIG. 3. Enthalpy of mixing ΔH_{mix} for the NM, AFM, and AFM+ U ($U = 1$ eV) configurations of CrVAIC ($x = 0.5$). Color code: SQSCrV (NM, red), VVCrCr(CrV)(VCr) (AFM and AFM+ U , red), VCrCrV (black), VCrCrV (green), and VVCrCr (blue). Lines without symbols: NM; with circles: AFM; with squares: AFM+ U . Here, AFM refers to the lowest-energy configuration among the AFM arrangements considered, as described in Table II.

for Cr_2AlC and the present calculations confirm this result. The ground state for V_2AlC was found to be NM [60]. We tested this by starting with the same spin options proposed for Cr_2AlC and found that V_2AlC relaxes into the NM state in all cases. For the equiatomic composition, all AFM, FM, and NM configurations consistent with the considered cell have been considered. The preferred state is found to be always an AFM state. Details of the preferred AFM spin configurations for the chemically ordered (VCrCrV, VCrVCr, and VVCrCr) and disordered [VVCrCr(CrV)(VCr)] structures are given in Appendix B. Figure 3 compares the formation enthalpies ΔH_{mix} of the AFM configurations with the NM configurations at $x = 0.5$. For the AFM calculations, both DFT and DFT+ U were considered, the latter using a value of $U = 1$ eV following previous work on Cr [38]. The NM results reproduce the values given in Fig. 2. It is clearly seen that the alloys become more unstable when magnetism is considered. Although magnetism and + U corrections tend to favor different chemically ordered structures, the disordered arrangements [SQSCrV for NM and VVCrCr(CrV)(VCr) for AFM and AFM+ U] always have the highest enthalpies and are the most unstable.

Figure 4(a) replots the enthalpies of mixing shown in Figs. 2 and 3 but also includes the $-T\Delta S_c$ curves for three equiatomic ($x = 0.5$) structures for the specific values of the temperature such that $T\Delta S_c = \Delta H_{\text{mix}}$ for the NM, AFM, and AFM+ U results, giving estimates of the stabilization temperature T_s for which $\Delta G_{\text{mix}} = 0$, and below which the mixed phase is therefore thermodynamically unstable. The chosen structures and magnetic configurations for the different cases are SQSCrV (NM), VVCrCr(CrV)(VCr) (AFM), and VVCrCr(CrV)(VCr) (AFM+ U) because these are the most unstable phases for this composition in each case (red lines in Fig. 3). The corresponding stabilization temperatures are $T_s = 142$, 516, and 654 K, respectively. Figure 4(b) focuses only on the $x = 0.5$ composition and includes the $-T\Delta S_c$ curve corresponding to the mean experimental

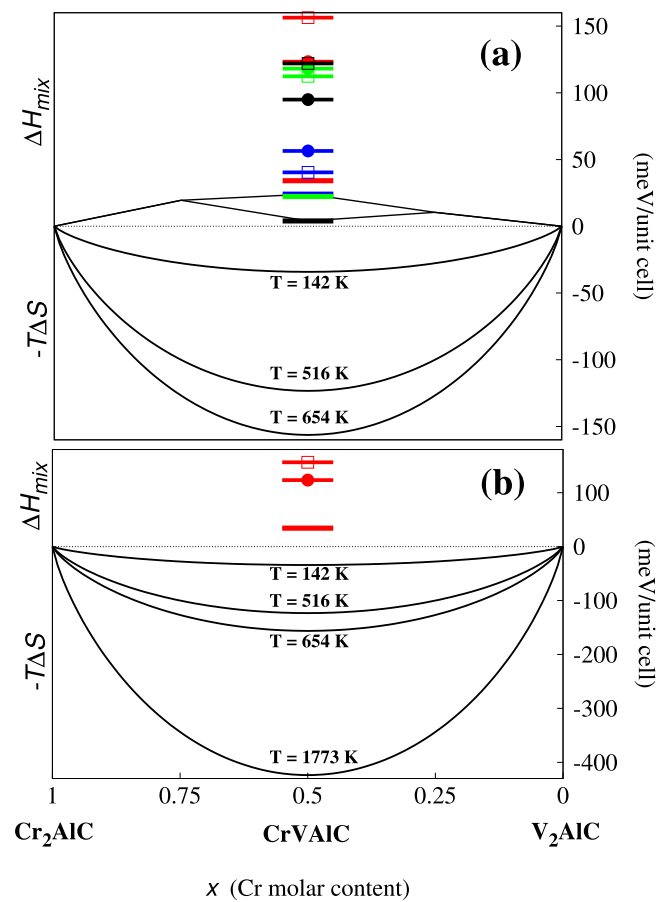


FIG. 4. (a) Enthalpy of mixing ΔH_{mix} for all chemically ordered and disordered structures of $(\text{Cr}_x, \text{V}_{1-x})_2\text{AlC}$ considered in this work as a function of x . The same color coding is used as in Figs. 2 and 3. Also shown are the $-T\Delta S_c$ curves for three equiatomic ($x = 0.5$) structures at the critical temperature when $T\Delta S_c$ is equal to ΔH_{mix} . The chosen structures, magnetic configurations, and temperatures are SQSCrV (NM, $T = 142$ K), VVCrCr(CrV)(VCr) (AFM, $T = 516$ K), and VVCrCr(CrV)(VCr) (AFM+ U , $T = 654$ K). (b) Same as (a) except only disordered structures (with the associated $-T\Delta S_c$ curves) are shown along with the curve for the mean experimental temperature ($T = 1773$ K).

temperature $T = 1773$ K [47]. Figure 5 shows ΔG_{mix} plotted as a function of temperature for the three equiatomic structures. At $T = 0$ K, the expression $\Delta G_{\text{mix}} = \Delta H_{\text{mix}}$ is recovered for the corresponding values of the enthalpy of mixing. When $\Delta G_{\text{mix}} = 0$, the expression $\Delta H_{\text{mix}} = T\Delta S_{\text{mix}}$ is obtained together with the critical temperatures.

It is thus predicted that the mixed phase $(\text{Cr}_{0.5}, \text{V}_{0.5})_2\text{AlC}$ is thermodynamically stable at temperatures higher than a stabilization temperature T_s estimated to be around 600 K. The DFT + U estimate is considered here to be probably the most accurate obtained in this work. The effect of introducing a + U term for this kind of material has been amply discussed in Refs. [36–38, 59, 72]. It provides well-defined magnetic moments for the Cr atoms, which is not the case for semilocal density functionals. However, higher levels of theory (beyond DFT, when amenable) should give more accurate estimates. We have chosen not to use hybrid functionals for this study.

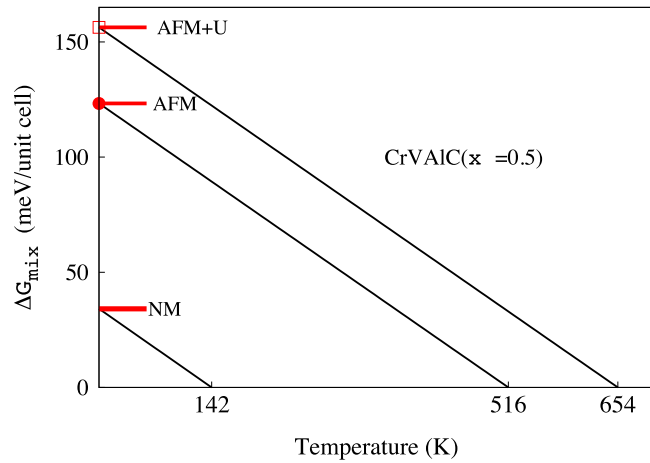


FIG. 5. Gibbs free energy of mixing ΔG_{mix} for NM, AFM, and AFM+ U configurations of CrVAIC ($x = 0.5$) as a function of temperature. ΔG_{mix} becomes zero at the corresponding critical temperatures.

Earlier work [36] on very closely related materials has shown no clear advantage over DFT + U , but rather the opposite in some cases. It should be remembered, however, that a more precise definition of T_s would require the explicit consideration of finite-temperature corrections to ΔE_{mix} , the inclusion of $p\Delta V_{\text{mix}}$ terms, and a more accurate calculation of ΔS_{mix} including vibrational contributions as well as correlation corrections to the configurational entropy, and spin disorder. It is clear, however, that, in spite of the low magnetic transition temperature measured for the Cr end member [56] of 73 K, which would seem to imply that magnetism would not be relevant at significantly higher temperatures, a model solution would give a rather poor estimate of $T_s = 142$ K, although reaching the same qualitative conclusion.

It is therefore expected that the mixed phases are stable at the synthesis conditions (as observed), and remain metastable when cooled down to room temperature for kinetic reasons. This scenario would also predict that if T_s is sufficiently high to allow significant diffusion when cooling well below this temperature, a tendency towards spinodal decomposition would exist, which might be observed if cooling sufficiently slowly. An estimation of the timescales relevant

TABLE I. Parameters for generating the Cr and V pseudopotentials for the two valence configurations fs and ss . The parameters used to generate the Al and C pseudopotentials are also given. $r_c(s, p, d$ or f) refer to the core radii for the orbitals (values are in bohr) and $s, d, p,$ and f are the corresponding electron occupancies. r_{core} is the radius for including partial core corrections [75].

		$r_c(s)$	$r_c(p)$	$r_c(d)$	$r_c(f)$	r_{core}	s	p	d	f
fs	Cr	2.80	1.70	2.50	2.25	1.85	1.0	6.0	5.0	0.0
	V	2.80	1.65	2.50	2.25	1.74	2.0	6.0	3.0	0.0
ss	Cr	1.00	1.60	2.50	2.25	1.38	2.0	6.0	5.0	0.0
	V	1.00	1.60	2.50	2.25	1.38	2.0	6.0	3.0	0.0
	Al	2.28	2.28	2.28	2.28	1.5	2.0	0.5	0.5	0.0
	C	1.25	1.25	1.25	1.25	1.6	2.0	2.0	0.0	0.0

for this phenomenon to be observed would require a more precise knowledge of T_s , and good estimates of the relevant diffusivities, which are beyond the scope of this work. For the configurational disorder that remains frozen in, however, the antiferromagnetic frustration already seen in the Cr end member (due to the hexagonal Cr layers) could give rise to interesting spin orderings when the Cr cations alternate with nonmagnetic V cations in a disordered fashion. The spin configurations shown in Table II are just a small sample of what less-ordered cation arrangements could produce, including ferrimagnetic response, plausibly involving spin canting.

IV. CONCLUSIONS

Using first-principles DFT calculations, the effect of temperature and magnetism on the stability of $(\text{Cr}_x\text{V}_{1-x})_2\text{AlC}$ MAX phases has been studied. At $T = 0$ K, calculations of the enthalpy of mixing indicate that chemically ordered structures across the composition range are unstable with respect to decomposition into the two end members. Further calculations at the equiatomic composition, CrVAIC ($x = 0.5$), show that the effect of chemical disorder does not change this conclusion, but tend to make the structures even more unstable. Calculations including different magnetic arrangements uphold this conclusion. However, when configurational entropy and magnetism are included, these disordered structures can be stabilized with temperature. It is found that at the equiatomic composition, the disordered structure VVCrCr(CrV)(VCr) is favored with an AFM stabilization temperature $T_s = 654$ K using DFT + U . Changing the level of theory (to DFT) or the nature of the disorder (to SQSCrV) reduces T_s , which nevertheless remains above absolute zero. Thus, although the measured Curie temperature of Cr_2AlC is about 73 K, the calculations predict that introducing vanadium can not only stabilize the quaternary phase at temperatures well below those typically used during synthesis, but also induce new magnetic arrangements. It is hoped that this work will stimulate new measurements of the magnetic properties of the $(\text{Cr}_x\text{V}_{1-x})_2\text{AlC}$ solid solution series.

ACKNOWLEDGMENTS

The authors gratefully acknowledge the computational resources from Marenostrum III and IV (Barcelona Supercomputer Center, Spain). E.A. thanks EC-FP7-PEOPLE-CIG-2012 Marie Curie, Project No. 333813 ElectronStopping of the European Union. P.D.B. and S.H.S. thank the Donostia International Physics Center (DIPC) and EPSRC Grant No. EP/M018768/1, respectively, for travel and subsistence during their visits.

APPENDIX A

Pseudopotentials for Cr and V have been generated using the program ATOM [73] considering the relativistic PBE [65] functional within the Troullier-Martins (tm2) [74] scheme. Basis sets for Cr and V, denoted DZP, DZP+P(3d), and TZ2P+P(3d), have been defined according to the valence configurations fs and ss . The parameters for Cr, V, Al, and C used in this work to generate the corresponding

TABLE II. Parameters for the basis sets DZP, DZP+P(3*d*), and TZ2P+P(3*d*) associated with the two valence configurations defined for Cr and V. $r_{1,2,or3}$ are cutoff radii (bohr) of each “zeta” for the orbital (orb). r_* is the internal radius of the soft confinement potential [76] (with $V_0=40$ Ry) while r_Q is the radius associated to the charge confinement potential [77].

	Cr basis						V basis												
	<i>fs</i>			<i>ss</i>			<i>fs</i>			<i>ss</i>									
	orb	r_1	r_2	r_3	r_*	r_Q	orb	r_1	r_2	r_3	r_*	r_Q	orb	r_1	r_2	r_3	r_*	r_Q	
DZP	3_p	10.0			8.5		3_s	10.0	2.5		8.5		3_p	10.0			8.5		
	3_d	10.0	3.0		8.5		3_p	10.0	2.5		8.5		3_d	10.0	3.0		8.5		
	4_s	10.0	3.0		8.5		3_d	10.0	3.0		8.5		4_s	10.0	3.0		8.5		
	4_p	10.0			8.5	1.3	4_s	10.0	3.0		8.5		4_p	10.0			8.5	1.3	
						4_p	10.0			8.5	1.38						8.5	1.38	
DZP+P(3 <i>d</i>)	3_p	10.0			8.5		3_s	10.0	2.5		8.5		3_p	10.0			8.5		
	3_d	10.0	3.0		8.5		3_p	10.0	2.5		8.5		3_d	10.0	3.0		8.5		
	4_f	10.0					3_d	10.0	3.0		8.5		4_f	10.0			8.5		
	4_s	10.0	3.0		8.5		4_f	10.0					4_s	10.0	3.0		8.5		
	4_p	10.0			8.5	1.3	4_s	10.0	3.0		8.5		4_p	10.0			8.5	1.3	
						4_p	10.0			8.5	1.38						8.5	1.38	
TZ2P+P(3 <i>d</i>)	3_p	10.0	4.0	3.0	9.0		3_s	10.0	3.5	2.5	9.0		3_p	10.0	4.0	3.0	9.0		
	3_d	10.0	4.0	3.0	9.0		3_p	10.0	3.5	2.5	9.0		3_d	10.0	4.0	3.0	9.0		
	4_f	10.0					3_d	10.0	4.0	3.0	9.0		4_f	10.0			9.0		
	4_s	10.0	4.0	3.0	9.0		4_f	10.0					4_s	10.0	4.0	3.0	9.0		
	4_p	10.0	3.0		9.0	1.3	4_s	10.0	4.0	3.0	9.0		4_p	10.0	3.0		9.0	1.3	
						4_p	10.0	3.0		9.0	1.38						9.0	1.38	

pseudopotentials are given in Table I while those for the basis sets are given in Tables II and III.

Figure 6 compares the calculated enthalpy of mixing of the NM state for the VVCrCr structure using the different basis sets and pseudopotentials. The physical situation remains the same regardless of the particular choice of basis or pseudopotential. The largest value of ΔH_{mix} over the composition range is obtained using the *ss* valence configuration and the DZP+P(3*d*) basis set. There is a difference of approximately 5 meV/unit cell between this choice and the one using the *fs* configuration (same basis). This difference is not large enough to have a significant effect on the overall results.

TABLE III. Parameters associated to Al and C basis sets are given. $r_{1,2,or3}$ are cutoff radii (bohr) of each “zeta” for the orbital (orb). r_* is the internal radius of the soft confinement potential [76] (with $V_0=40$ Ry) while r_Q is the radius associated to the charge confinement potential [77].

	orb	r_1	r_2	r_*	r_Q
Al basis	3_s	10.0	4.0	8.0	
	3_p	10.0	5.0	8.0	
	3_d	10.0		8.0	2.5 0.0
C basis	2_s	10.0	3.0	8.0	
	2_p	10.0	2.8	8.0	
	3_d	10.0		8.0	9.6 0.7

APPENDIX B

The GGA+*U* calculations were performed using a value of $U = 1$ eV for the Cr 3*d* electrons. The LDA+*U* projectors were generated as slightly excited numerical atomic orbitals [78] with a radius orbital of 2.3 bohr along with a population and threshold tolerance of 0.0004 and 0.02, respectively. AFM spin arrangements for $2 \times 1 \times 1$ chemically ordered structures and for VVCrCr(CrV)(VCr) are shown in Table IV along with the corresponding electron populations with and without +*U* corrections.

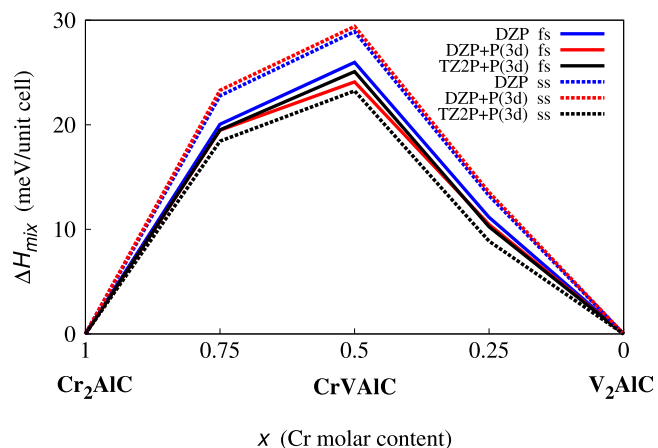
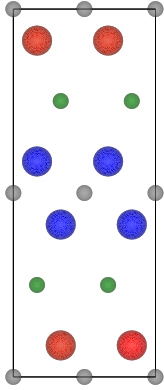
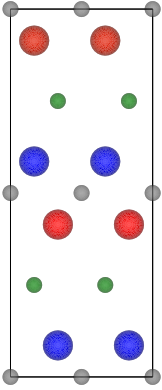
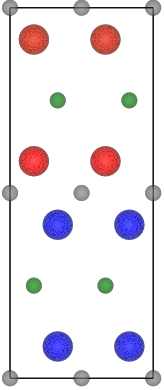
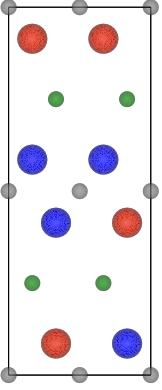



FIG. 6. Enthalpy of mixing ΔH_{mix} of the VVCrCr (NM) structure as a function of x , basis, and pseudopotential.

TABLE IV. $2 \times 1 \times 1$ supercell structures for $(\text{Cr}_{0.5}\text{V}_{0.5})_2\text{AlC}$ denoted VCrCrV, VCrVCr, VVCrCr, and VVCrCr(CrV)(VCr). The vertical direction points along the c axis. The table gives the Mulliken spin population difference [79] $n_{i\uparrow} - n_{i\downarrow}$ for atom i and is listed in the same order along the c axis as shown in the structures. These values were obtained for AFM spin arrangements and for the same spin arrangements with $+U$ corrections on the Cr atoms. Even though the $+U$ corrections did not affect the AFM arrangements for chemically ordered structures, for VVCrCr(CrV)(VCr) the spin arrangement changed to ferrimagnetic with a net magnetic moment given by 0.46 electrons.

				
	2x1x1 VCrCrV	2x1x1 VCrVCr	2x1x1 VVCrCr	VVCrCr(CrV)(VCr)
AFM	-0.10 V +0.10 V -0.88 Cr +0.88 Cr +0.88 Cr -0.88 Cr +0.10 V -0.10 V	+0.01 V -0.01 V +0.08 Cr -0.08 Cr +0.01 V -0.01 V +0.08 Cr -0.08 Cr	-0.02 V +0.02 V -0.02 V +0.02 V +1.39 Cr -1.39 Cr +1.39 Cr -1.39 Cr	+0.04 V -0.16 V +0.52 Cr -0.67 Cr -1.26 Cr +0.19 V -0.24 V +0.77 Cr
AFM+U	-0.24 V +0.24 V -2.19 Cr +2.19 Cr +2.19 Cr -2.19 Cr +0.24 V -0.24 V	+0.30 V -0.30 V +2.51 Cr -2.51 Cr +0.30 V -0.30 V +2.51 Cr -2.51 Cr	-0.03 V +0.03 V -0.03 V +0.03 V +2.36 Cr -2.36 Cr +2.36 Cr -2.36 Cr	+0.36 V -0.32 V +2.12 Cr -2.46 Cr -2.25 Cr +0.31 V -0.43 V +2.21 Cr
	 Cr V Al C			

- [1] M. W. Barsoum, *MAX Phases: Properties of Machinable Ternary Carbides and Nitrides* (Wiley, Hoboken, NJ, 2013).
- [2] M. W. Barsoum, *Prog. Solid State. Chem.* **28**, 201 (2000).
- [3] P. Eklund, M. Beckers, U. Jansson, H. Högborg, and L. Hultman, *Thin Solid Films* **518**, 1851 (2010).
- [4] P. Eklund, J. Rosen, and P. O. A. Persson, *J. Phys. D: Appl. Phys.* **50**, 113001 (2017).
- [5] T. Lapauw, B. Tunca, T. Cabioch, J. Lu, P. Persson, K. Lambrou, and J. Vleugels, *Inorg. Chem.* **55**, 10922 (2016).
- [6] T. Lapauw, K. Lambrou, T. Cabioch, J. Halim, J. Lu, A. Pesach, O. Rivin, O. Ozeri, E. Caspi, L. Hultman *et al.*, *J. Eur. Ceram. Soc.* **36**, 1847 (2016).
- [7] T. Lapauw, J. Halim, J. Lu, T. Cabioch, L. Hultman, M. Barsoum, K. Lambrou, and J. Vleugels, *J. Eur. Ceram. Soc.* **36**, 943 (2016).
- [8] T. Lapauw, B. Tunca, T. Cabioch, J. Vleugels, and K. Lambrou, *J. Eur. Ceram. Soc.* **37**, 4539 (2017).
- [9] H. Fashandi, M. Dahlqvist, J. Lu, J. Palisaitis, S. Simak, I. Abrikosov, J. Rosen, L. Hultman, M. Andersson, A. Spetz *et al.*, *Nat. Mater.* **16**, 814 (2017).
- [10] Z. M. Sun, *Intern. Mater. Rev.* **56**, 143 (2011).
- [11] M. W. Barsoum, H.-I. Yoo, I. K. Polushina, V. Y. Rud, Y. V. Rud, and T. El-Raghy, *Phys. Rev. B* **62**, 10194 (2000).
- [12] D. Li, Y. Liang, X. Liu, and Y. Zhou, *J. Eur. Ceram. Soc.* **30**, 3227 (2010).
- [13] M. Radovic and M. W. Barsoum, *Am. Ceram. Soc. Bull.* **92**, 20 (2013).
- [14] H. B. Zhang, Y. C. Zhou, Y. W. Bao, and M. S. Li, *J. Mater. Res.* **21**, 2401 (2006).
- [15] J. Wang and Y. Zhou, *Ann. Rev. Mater. Res.* **39**, 415 (2009).
- [16] Z. J. Lin, M. S. Li, J. Y. Wang, and Y. C. Zhou, *Acta Mater.* **55**, 6182 (2007).
- [17] T. Zhen, M. W. Barsoum, S. R. Kalidindi, M. Radovic, Z. M. Sun, and T. El-Raghy, *Acta Mater.* **53**, 4963 (2005).
- [18] X. H. Wang and Y. C. Zhou, *Corrosion Sci.* **45**, 891 (2003).
- [19] X. K. Qian, X. D. He, Y. B. Li, Y. Sun, H. Li, and D. L. Xu, *Corrosion Sci.* **53**, 290 (2011).
- [20] D. W. Clark, S. J. Zinkle, M. K. Patel, and C. M. Parish, *Acta Mater.* **105**, 130 (2016).
- [21] E. N. Hoffman, D. W. Vinson, R. L. Sindelar, D. J. Tallman, G. Kohse, and M. W. Barsoum, *Nucl. Eng. Design* **244**, 17 (2012).
- [22] T. R. Allen, R. J. M. Konings, and A. T. Motta, *Comprehensive Nucl. Mater.* **5**, 49 (2012).

- [23] A. S. Ingason, M. Dahlqvist, and J. Rosen, *J. Phys.: Condens. Matter* **28**, 433003 (2016).
- [24] M. Magnuson and M. Mattesini, *Thin Solid Films* **621**, 108 (2017).
- [25] W. Luo and R. Ahuja, *J. Phys.: Condens. Matter* **20**, 064217 (2008).
- [26] M. Dahlqvist and J. Rosen, *Phys. Chem. Chem. Phys.* **17**, 31810 (2015).
- [27] A. Mockute, J. Lu, E. J. Moon, M. Yan, B. Anasori, S. J. May, M. Barsoum, and J. Rosen, *Mater. Res. Lett.* **3**, 16 (2015).
- [28] A. S. Ingason, A. Petruhins, M. Dahlqvist, F. Magnus, A. Mockute, B. Alling, L. Hultman, I. A. Abrikosov, P. O. Å. Persson, and J. Rosen, *Mater. Res. Lett.* **2**, 89 (2014).
- [29] Z. Liu, T. Waki, Y. Tabata, K. Yuge, H. Nakamura, and I. Watanabe, *Phys. Rev. B* **88**, 134401 (2013).
- [30] C. C. Lai, A. Petruhins, J. Lu, M. Farle, L. Hultman, P. Eklund, and J. Rosen, *Mater. Res. Lett.* **5**, 533 (2017).
- [31] C. C. Lai, Q. Tao, H. Fashandi, U. Wiewald, R. Salikhov, M. Farle, A. Petruhins, J. Lu, L. Hultman, P. Eklund, and J. Rosen, *APL Mater.* **6**, 026104 (2018).
- [32] Z. Sun, R. Ahuja, S. Li, and J. M. Schneider, *Appl. Phys. Lett.* **83**, 899 (2003).
- [33] J. Wang and Y. Zhou, *Phys. Rev. B* **69**, 214111 (2004).
- [34] J. D. Hettinger, S. E. Lofland, P. Finkel, T. Meehan, J. Palma, K. Harrell, S. Gupta, A. Ganguly, T. El-Raghy, and M. W. Barsoum, *Phys. Rev. B* **72**, 115120 (2005).
- [35] B. Manoun, R. P. Gulve, S. K. Saxena, S. Gupta, M. W. Barsoum, and C. Z. Zha, *Phys. Rev. B* **73**, 024110 (2006).
- [36] M. Ramzan, S. Lebègue, and R. Ahuja, *Phys. Status Solidi: Rapid Res. Lett.* **5**, 122 (2011).
- [37] M. Dahlqvist, B. Alling, and J. Rosen, *J. Appl. Phys.* **113**, 216103 (2013).
- [38] M. Dahlqvist, B. Alling, and J. Rosen, *J. Phys.: Condens. Matter* **27**, 095601 (2015).
- [39] S. Lin, P. Tong, B. S. Wang, Y. N. Huang, W. J. Lu, D. F. Shao, B. C. Zhao, W. H. Song, and Y. P. Sun, *J. Appl. Phys.* **113**, 053502 (2013).
- [40] S. Lin, Y. Huang, L. Zu, X. Kan, J. Lin, W. Song, P. Tong, X. Zhu, and Y. Sun, *J. Alloys Compounds* **680**, 452 (2016).
- [41] O. Rivin, E. N. Caspi, A. Pesach, H. Shaked, A. Hoser, R. Georgii, Q. Tao, J. Rosen, and M. W. Barsoum, *Mater. Res. Lett.* **5**, 465 (2017).
- [42] R. Salikhov, A. S. Semisalova, A. Petruhins, A. S. Ingason, J. Rosen, U. Wiedwald, and M. Farle, *Mater. Res. Lett.* **3**, 156 (2015).
- [43] A. Mockute, P. O. Å. Persson, F. Magnus, A. S. Ingason, S. Olafsson, L. Hultman, and J. Rosen, *Phys. Status Solidi: Rapid Res. Lett.* **8**, 420 (2014).
- [44] M. Dahlqvist, B. Alling, I. A. Abrikosov, and J. Rosen, *Phys. Rev. B* **84**, 220403 (2011).
- [45] Z. Liu, T. Waki, Y. Tabata, and H. Nakamura, *Phys. Rev. B* **89**, 054435 (2014).
- [46] A. S. Ingason, A. Mockute, M. Dahlqvist, F. Magnus, S. Olafsson, U. B. Arnalds, B. Alling, I. A. Abrikosov, B. Hjörvarsson, P. O. A. Persson, and J. Rosen, *Phys. Rev. Lett.* **110**, 195502 (2013).
- [47] J. Halim, P. Chartier, T. Basyuk, T. Prikhna, E. N. Caspi, M. W. Barsoum, and T. Cabioch, *J. Eur. Ceram. Soc.* **37**, 15 (2017).
- [48] E. N. Caspi, P. Chartier, F. Porcher, F. Damay, and T. Cabioch, *Mater. Res. Lett.* **3**, 100 (2015).
- [49] J. Schuster, H. Nowotny, and C. Vaccaro, *J. Solid State Chem.* **32**, 213 (1980).
- [50] Y. Zhou, F. Meng, and J. Zhang, *J. Am. Ceram. Soc.* **91**, 1357 (2008).
- [51] L. Shang, D. Music, M. to Baben, and J. M. Schneider, *J. Phys. D: Appl. Phys.* **47**, 065308 (2014).
- [52] M. Dahlqvist, B. Alling, and J. Rosen, *Phys. Rev. B* **81**, 220102 (2010).
- [53] S. H. Shah and P. D. Bristowe, *Sci. Rep.* **7**, 9667 (2017).
- [54] H. Han, D. Wickramaratne, Q. Huang, J. Dai, T. Li, H. Wang, W. Zhang, and P. Huai, *RSC Adv.* **6**, 84262 (2016).
- [55] C. Wang, T. Yang, J. Xiao, S. Liu, J. Xue, Q. Huang, J. Zhang, J. Wang, and Y. Wang, *J. Am. Ceram. Soc.* **99**, 1769 (2016).
- [56] M. Jaouen, P. Chartier, T. Cabioch, V. Mauchamp, G. André, and M. Viret, *J. Am. Ceram. Soc.* **96**, 3872 (2013).
- [57] M. Jaouen, M. Bugnet, N. Jaouen, P. Ohresser, V. Mauchamp, T. Cabioch, and A. Rogalev, *J. Phys.: Condens. Matter* **26**, 176002 (2014).
- [58] J. M. Schneider, Z. Sun, R. Mertens, F. Uestel, and R. Ahuja, *Solid State Commun.* **130**, 445 (2004).
- [59] J. Wang, Z. Liu, H. Zhang, and J. Wang, *J. Am. Ceram. Soc.* **99**, 3371 (2016).
- [60] J. M. Schneider, R. Mertens, and D. Music, *J. Appl. Phys.* **99**, 013501 (2006).
- [61] C. M. Hamm, M. Dürrschnabel, L. Molina-Luna, R. Salikhov, D. Spoddig, M. Farle, U. Wiedwald, and C. S. Birkel, *Mater. Chem. Front.* **2**, 483 (2018).
- [62] P. Hohenberg and W. Kohn, *Phys. Rev.* **136**, B864 (1964).
- [63] W. Kohn and L. J. Sham, *Phys. Rev.* **140**, A1133 (1965).
- [64] J. M. Soler, E. Artacho, J. D. Gale, A. García, J. Junquera, P. Ordejón, and D. Sánchez-Portal, *J. Phys.: Condens. Matter* **14**, 2745 (2002).
- [65] J. P. Perdew, K. Burke, and M. Ernzerhof, *Phys. Rev. Lett.* **77**, 3865 (1996).
- [66] M. R. Hestenes and E. Stiefel, *J. Res. Natl. Bureau Stand.* **49**, 409 (1952).
- [67] J. Moreno and J. M. Soler, *Phys. Rev. B* **45**, 13891 (1992).
- [68] A. Zunger, S.-H. Wei, L. G. Ferreira, and J. E. Bernard, *Phys. Rev. Lett.* **65**, 353 (1990).
- [69] S. L. Dudarev, G. A. Botton, S. Y. Savrasov, C. J. Humphreys, and A. P. Sutton, *Phys. Rev. B* **57**, 1505 (1998).
- [70] B. Fultz, *Prog. Mater. Sci.* **55**, 247 (2010).
- [71] B. Fultz, L. Anthony, J. L. Robertson, R. M. Nicklow, S. Spooner, and M. Mostoller, *Phys. Rev. B* **52**, 3280 (1995).
- [72] M. Mattesini and M. Magnuson, *J. Phys.: Condens. Matter* **25**, 035601 (2013).
- [73] A. García, ATOM Pseudopotential generation program, <http://www.siesta-project.org/Pseudopotentials>
- [74] N. Troullier and J. L. Martins, *Phys. Rev. B* **43**, 1993 (1991).
- [75] S. G. Louie, S. Froyen, and M. L. Cohen, *Phys. Rev. B* **26**, 1738 (1982).
- [76] J. Junquera, Ó. Paz, D. Sánchez-Portal, and E. Artacho, *Phys. Rev. B* **64**, 235111 (2001).
- [77] F. Corsetti, M. V. Fernández-Serra, J. M. Soler, and E. Artacho, *J. Phys.: Condens. Matter* **25**, 435504 (2013).
- [78] S. J. Riikonen, Ph.D. thesis, University of the Basque Country, EHU-UPV, San Sebastian, Spain, 2007, http://cfm.ehu.es/view/files/thesis_Sampsa_Riikonen.pdf
- [79] R. S. Mulliken, *J. Chem. Phys.* **23**, 1833 (1955).